ELECTROCHEMICAL BEHAVIOUR OF CARBON DIOXIDE ON PLATINUM AND RHODIUM

Martins, M.E.

Instituto de Investigaciones Fisicoquímicas Teóricas y Aplicadas (INIFTA),
Facultad de Ciencias Exactas, Universidad Nacional de La Plata,
Sucursal 4, CC 16 (1900), La Plata, Argentina.
Fax: +54-221-425-4642, E-mail : mmartins@inifta.unlp.edu.ar

Received August16th, 2005. In final form September 14th, 2005.

Dedicated to the memory of the late Prof. Hans J. Schumacher on the occasion of his 100th birthday

Abstract

The electroadsorption and electroreduction of carbon dioxide, and the subsequent electrooxidation of reduced carbon dioxide was studied on polycrystalline and electrofaceted Pt and on polycrystalline Rh electrodes. The influence of the adsorption potential and the adsorption time was established. Combining voltammetric charge measurements and differential electrochemical mass spectrometry (DEMS) analysis, three adsorbates were tentatively identified, namely COOH and CO in bridge and linear configurations on Pt, and COH in triple and single adsorption configurations on Rh. By applying medium frequency potential routines on the Pt-adsorbate/sulphuric acid interface, the existence of equilibrium between adsorbates was demonstrated.

Resumen

Se estudia la electroadsorción y la electrorreducción de dióxido de carbono como así también la electrooxidación del dióxido de carbono reducido sobre Pt policristalino y electrofacetado y sobre Rh policristalino. Se determina la influencia del potencial y del tiempo de adsorción. Mediante el empleo de técnicas combinadas voltamperométricas y de espectrometría de masa diferencial (DEMS), se identificaron tres adsorbatos posibles sobre Pt, COOH y CO en configuración lineal y puente, y dos sobre Rh, COH en configuraciones de adsorción simple y triple. Mediante la aplicación de perturbaciones de potencial a la interfase Pt-adsorbato/ácido sulfúrico acuoso, se demuestra la existencia de un equilibrio entre los adsorbatos.

Introduction

The electrochemical behaviour of several C_1-containing organic molecules shares some similarities that encourage the search of a molecular model for these compounds. However, the concept of molecular model should be strictly defined in order to be used for generalized purposes. For example, CO can be considered as a molecular model regarding electroadsorption processes, since, once it is adsorbed onto a metallic surface, the chemical structure remains unaltered and

only acquires different surface configurations, i.e., on top, bridge and multiple states [1-5]. In contrast, those C_1-containing molecules in which C atom exhibits a higher oxidation state than CO (carbon dioxide, formaldehyde), the formation of adsorbates on the metallic surface is assisted by H ad-atoms [6-8]. The chemical structure of these adsorbates is different from the original molecule, indicating that the electroadsorption process differs from that observed for CO.

Carbon dioxide can be considered as a molecular model by itself, because is the only carbonaceous substance with the C atom in the highest oxidation state (+4). Moreover, from an electrocatalytic point of view, carbon dioxide could be also considered as a molecular model for the electroadsorption process taking into account the nature of the adsorbed residues, which are similar to those of other C_1-containing compounds. There is wide experimental evidence that supports such assumptions. Several infrared spectroscopic studies allow to conclude that the main adsorbate formed from CO_2 [9-13] and other C_1-containing compounds [1,13-20] is CO with different surface configurations. Besides, selecting accurately the potential value of the modulation, COOH and COH adsorbates have been also identified [13-15]. However, transient electrochemical techniques such as voltammetry and coupled voltammetry/DEMS usually conclude that COH is the main adsorbate [16].

Therefore, those results suggest that, according to the experimental conditions, that different adsorbates can be formed. The experimental set up for infrared studies includes a thin layer configuration that favours the formation of CO, which is a thermodynamically stable product. On the other hand, DEMS analysis detects the first product, i.e., the one formed under kinetic control, because the reaction species formed at the surface of the electrode are detected on a very short time scale. Moreover, voltammetry allows predetermining the adsorption time and consequently to recognize adsorbates which were formed through either thermodynamic or kinetic control. Hence, low adsorption times favour the product initially formed and for prolonged adsorption times prevails the formation of thermodynamically stable adsorbates. As a result, cyclic voltammetry comes out as a useful technique to determine the conditions under which the adsorbates are formed. The occurrence of different adsorbates suggests the existence of equilibrium among them, the equilibrium position being dependent on the experimental conditions.

The aim of this work is to study the formation of reduced CO_2 adsorbates (r-CO_2) on platinum and rhodium, and to determine the possible relations between them.

Experimental

Electrochemical measurements were made by using a conventional glass-made electrochemical cell with Pt and Rh as working electrodes, large gauzes of Pt and Rh as counter electrodes, and a reversible hydrogen electrode as the reference. Potentials in the text are given on the reversible hydrogen electrode (RHE) scale.

Polycrystalline Pt and Rh wires were cleaned in hot $H_2SO_4 + HNO_3$ mixture, and cycled at 0.05 V s^{-1} from 0.05 to 1.50 V for Pt and from 0.02 to 1.40 V for Rh. For some experiments, preferentially oriented (electrofaceted) Pt surfaces were used and prepared employing potential routines that are thoroughly described elsewhere [6]. The real surface area of the electrodes was evaluated from the H-atom electrosorption charge. For this purpose, the H-adatom monolayer charge density for Pt and Rh surfaces was taken from the literature to be 210 $\mu C\ cm^{-2}$.

1 M aqueous H_2SO_4 (base electrolyte), deoxygenated by bubbling high purity nitrogen gas, and 1 M aqueous H_2SO_4 saturated with CO_2 (working solution) were prepared from analytical reagent quality chemicals and Millipore-Milli-Q* water. All runs were performed at 298 K under a nitrogen atmosphere.

For electroadsorption experiments, carbon dioxide was bubbled into the supporting electrolyte for 30 min while the platinum working electrode was subjected to a potential cycling from 0.05 to 1.45 V at 0.1 Vs^{-1}. Carbon dioxide adsorption on platinum was accomplished by holding the potential at the adsorption value E_{ad}, ($0.05 \leq E_{ad} \leq 0.35$) V for a period, t_{ad}, ($0 \leq t_{ad} \leq 600$ s), followed by nitrogen bubbled through the electrolyte to remove carbon dioxide. Subsequently, a negative going potential scan from E_{ad} to the cathodic switching potential, E_{cs} = 0.05 V followed by a positive going potential scan to the anodic switching potential, E_{as} = 1.45 V at 0.1 Vs^{-1} were applied. Carbon dioxide adsorbates generated at E_{ad} were oxidized during the positive going potential scan to E_{as}.

On the other hand, carbon dioxide adsorption on rhodium was accomplished at E_{ad} ($-0.35 \leq E_{ad} \leq 0.05$ V) for a period t_{ad} ($0 \leq t_{ad} \leq 900$ s). Taking into account that E_{ad} was located within a potential domain where the hydrogen evolution reaction takes place, a potential step to E = 0.25 V during 5 min was applied accompanied by nitrogen bubbling within the electrolyte to displace carbon dioxide. Afterwards, the oxidation of carbon dioxide adsorbates was performed by means of a positive going potential scan up to E_{as} = 1.4 V at 0.1 Vs^{-1}.

Differential Electrochemical Mass Spectrometry (DEMS) experiments were carried out in a 2 mL flow cell. Rh working electrode was electrodeposited at a constant potential onto a substrate constructed with a hydrophobic PTFE membrane (Scimat Ltd., porous size 17 μm, 50 % porosity) covered with a gold deposit, employing a solution containing 3 % $RhCl_3$ in 1 M HCl. The mass signal m/z = 44 ($[CO2]^{\bullet+}$) corresponding to CO_2 was followed during the oxidation of the adsorbates. Details on the procedure for the calibration of DEMS systems are thoroughly described elsewhere [17].

Medium frequency potential routine (MFPR) involving a repetitive triangular potential cycling run at a sweep rate equal to 2 Vs^{-1} was applied to an electrofaceted Pt surface previously covered by r-CO_2 adsorbates. The potential domain of the MFPR corresponded to that of the OH-electrosorption reaction.

Results

General features of voltammograms of r-CO_2 on Pt and Rh

The voltammograms shown in Figure 1a, exhibit a current peak at 0.82 V and a shoulder at 0.73 V corresponding to the oxidation of r-CO_2 adsorbates generated on Pt within the potential range from 0.05 to 0.35 V for an adsorption time ($30 \leq t_{ad} \leq 600$) s. For potentials higher than 0.95 V, the electro-oxidation current and that of the blank are identical, hence at this potential the complete desorption of r-CO_2 has been achieved. The amount of r-CO_2, which has been calculated from the electrooxidation charge density, varies with E_{ad} (Figure 1b). For $E_{ad} \leq 0.15$ V, a maximum constant charge density of 194 μCcm^{-2} is found, while for $E_{ad} > 0.15$ V, a fast decrease of the amount of adsorbate is observed. Likewise, the influence of t_{ad} was studied at E_{ad} = 0.10 V (Figure 1c), and for t_{ad} = 300 s the maximum coverage is attained.

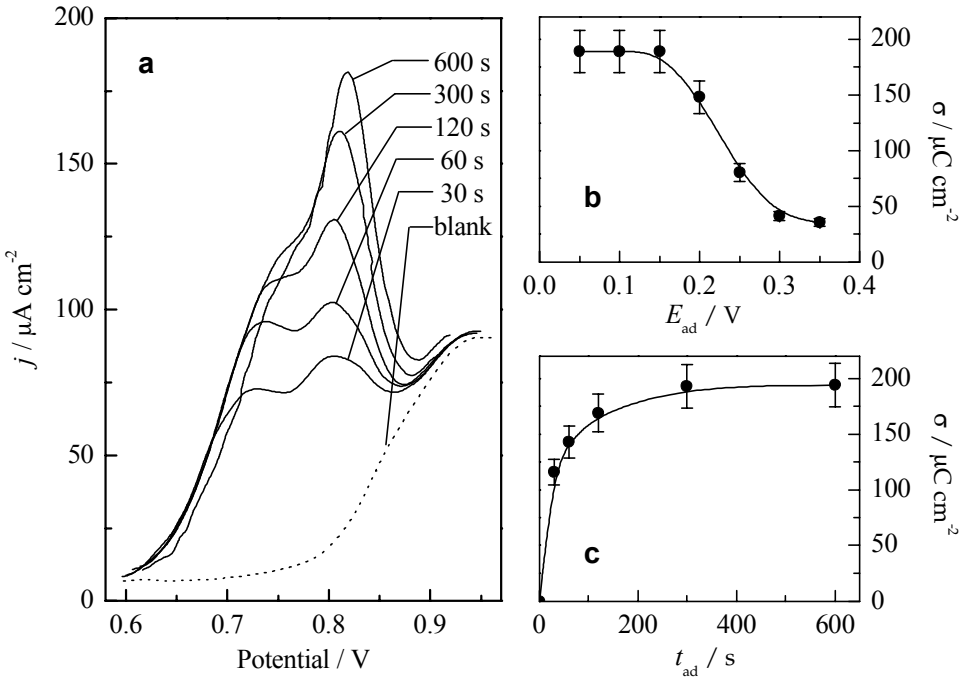

***Figure 1**. a) Voltammograms of pc Pt in working solution after E_{ad} = 0.10 V for 30 ≤ t_{ad} ≤ 600 s; v = 0.1 V s^{-1}; b) Charge density vs E_{ad} plot for t_{ad} = 300 s; c) Charge density vs t_{ad} plot at E_{ad} = 0.10 V.*

To gain information about the r-CO_2 adsorbates, the anodic part of the voltammograms performed at E_{ad} after different t_{ad} were graphically deconvoluted. The results are depicted in Figure 2a where three contributions, namely AIII (0.68 – 0.70 V), AI (0.73 – 0.77 V) and AII (0.80 - 0.82 V) can be distinguished. The evolution of charge density with t_{ad} for each contribution (Figure 2b) shows that AI steadily increases up to 300 s, while both AIII and AII display a maximum at ca. 100 s and thereafter decrease either to a constant finite value (AII) or to a null value (AIII).

On the other hand, the voltammogram for the electro-oxidation of r-CO_2 on Rh is less clearly defined than that on Pt because of the overlapping of the early stages of O-electroadsorption, which occur at a potential lower than that of Pt. An electro-oxidation current peak corresponding to r-CO_2 is observed at 0.78 V (Figure 3a). The maximum amount of adsorbate is achieved at high negative values of E_{ad} and for prolonged t_{ad} values (Figure 3b).

DEMS analysis of the electrooxidation product formed on Rh

The electrooxidation of r-CO_2 formed at E_{ad} = 0 V for t_{ad} = 10 min in 0.5 M aqueous H_2SO_4 was followed by DEMS (Figure 4, dashed line), monitoring the signal corresponding to the production of CO_2 (m/z = 44). It is not possible to perform this study at E_{ad} < 0 V, since the hydrogen evolution reaction brings about instability of Rh-deposited electrode. The electrooxidation of r-CO_2 begins at 0.50 V and a current peak at 0.70 V is developed. The oxidation charge density related to the latter process is equal to 141 μCcm^{-2}, and that associated to H electrodesorption results equal to 102 μCcm^{-2}. From these figures, a value for e.p.s. (number of

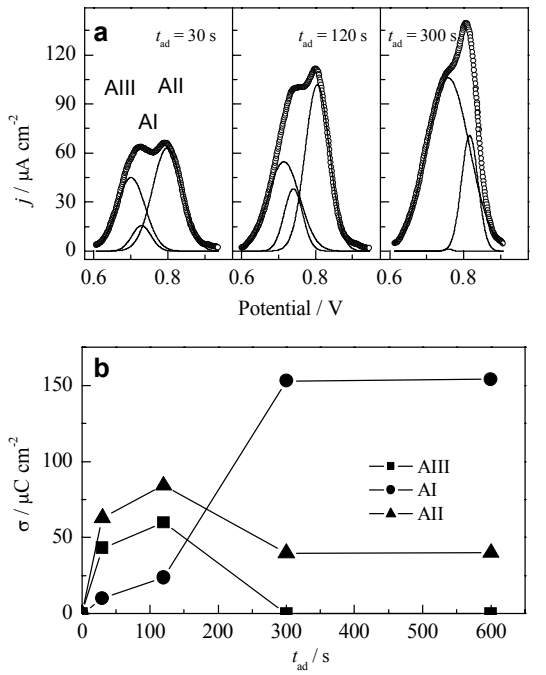

Figure 2. *a) Anodic voltammograms of pc Pt in working solution after E_{ad} = 0.10 V for t_{ad} = 30, 120 and 300 s, (O) experimental data (—) deconvoluted voltammograms showing components AI, AII, AIII; b) Charge density vs t_{ad} plot for components AI, AII, AIII depicted in a) v = 0.1 V s^{-1}.*

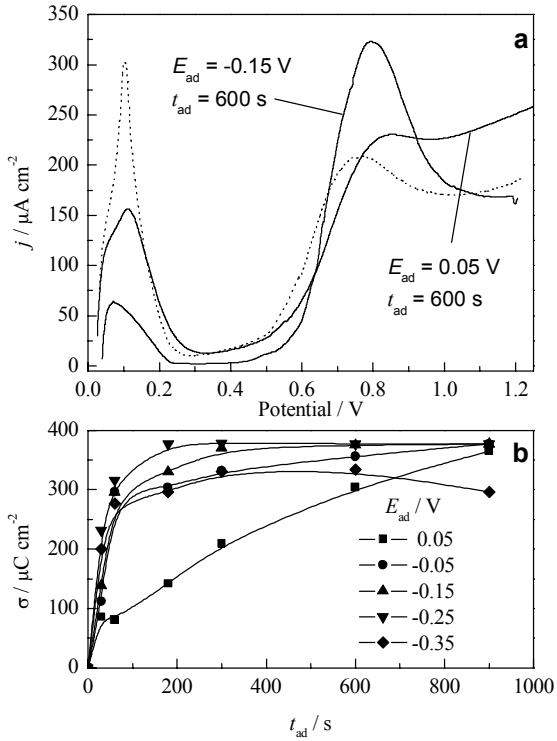

Figure 3. *a) Voltammograms of pc Rh in working solution after E_{ad} = -0.15 V and 0.05 V for t_{ad} = 600 s; (……) blank; b) Charge density vs t_{ad} plot for –0.35 ≤ E_{ad} ≤ 0.05 V. v = 0.1 Vs^{-1}.*

electrons per site) = 1.3 was calculated. Furthermore, from the massograms for the signal m/z = 44, the value of n (number of electrons) consumed to form one molecule of CO_2 is 2.97 (≈ 3). Consequently, from *e.p.s.* and n data, the number of Rh sites occupied was found to be 2.3.

For the sake of comparison, the electro-oxidation of CO was then performed at E_{ad} = 0.02 V for t_{ad} = 10 min in the same supporting electrolyte (Figure 4, dotted line). In this case, the current peak also starts at 0.50 V, but the maximum is reached at 0.63 V, involving an oxidation charge density of 318 μCcm^{-2}. The oxidation charge related to H electrodesorption was 57 μCcm^{-2}, yielding a value of *e.p.s.* of 2.1. The number of electrons was found to be 2, indicating that one site of Rh is occupied by adsorbed CO.

A proposal for identification of the adsorbates

A proposal for the identification of the adsorbates was encouraged, based specifically on *e.p.s*. values, the voltammetric behaviour, as well as a comparison of our results to those found in the literature concerning spectroscopic studies [15,21]. The results are resumed in Table 1.

Table 1 *Identification of adsorbates*

Adsorbate	AI	AII	AIII
Assignment	CO_L	CO_B	COOH

Where CO_L and CO_B correspond to linear and bridge configurations, respectively, of adsorbed CO.

Assessment of the surface equilibrium between adsorbates

The relative contribution of each adsorbate depends on the crystallographic sites of the electrode surface [11]. At high Miller index orientations, as those obtained by electrochemical faceting, CO_B species are mainly formed on (100) sites, while CO_L is the preferred intermediate on (110) terraces [18]. It has been previously shown that, on a preferentially oriented surface exhibiting (110) sites, all three r-CO_2 adsorbates are detected simultaneously [6]. Hence, the results indicate that electrofaceted surfaces can be appropriate substrates to account for the existence of a surface equilibrium between the adsorbates.

To carry out this study, CO_2 was allowed to react at E_{ad} = 0.20 V for 300 s on a Pt electrofaceted surface exhibiting a Pt(320) structure [22]. Once the CO_2 residues have been formed, a medium frequency potential routine (MFPR) was applied at f = 5 Hz in the (0.70 – 0.90) V potential domain, the stripping performance being compared with that obtained without application of the routine (Figure 5a). The comparison between the deconvoluted stripping profile without (Figure 5b) and with (Figure 5c) the use of the MFPR indicates that a redistribution of the adsorbates has taken place.

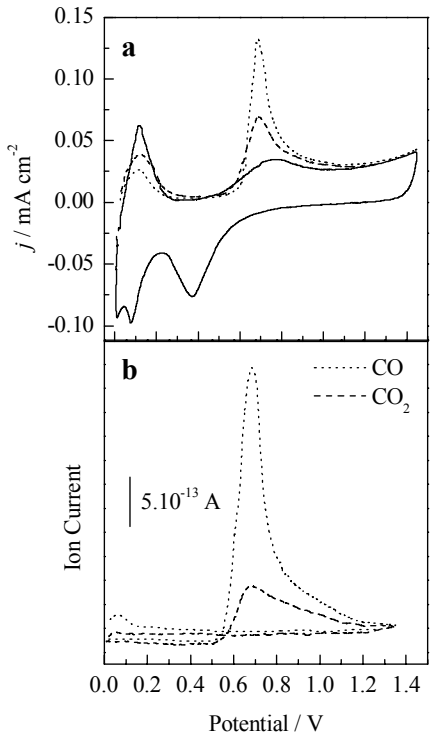

Figure 4. *a) Voltammograms of pc Rh showing the electro-oxidation of (…) CO adsorbates after E_{ad} = 0.02 V and (-----) CO_2 adsorbates after E_{ad} = 0 V for t_{ad} = 10 min, (—) blank. b) Simultaneous massograms of pc Rh under the same conditions as a). m/e = 44. v = 0.01 Vs^{-1}.*

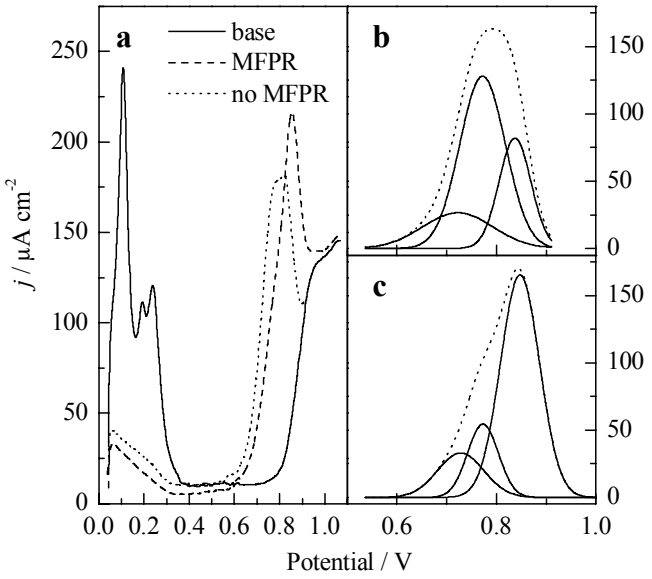

Figure 5. *a) Voltammograms of electrofaceted Pt in working solution after E_{ad} = 0.20 V for t_{ad} = 300 s; (----) with MFPR, (…) without MFPR, (—) blank. b) (—) Deconvoluted voltammogram without MFPR, (…) experimental data; c) (—) Deconvoluted voltammogram with MFPR, (…) experimental data. v = 0.1 Vs^{-1}.*

Discussion

Carbon dioxide electroadsorption on Pt and Rh

It is widely recognized that the formation r-CO_2 adsorbates from CO_2 is assisted by H adatoms [7,23,24] and that these adsorbates do not cover entirely the surface. For both metals, Pt and Rh, the largest amount of r-CO_2 is produced at potentials more negatives than the potential of zero charge, E_{pzc} (0.20 V for Pt and 0.00 V for Rh) [25]. In fact, E_{pzc} plays a key role in the electroadsorption process, as for $E > E_{pzc}$ the amount of r-CO_2 decreases remarkably. For $E = E_{pzc}$, CO_2 molecules approach the metallic surface without adsorption. Already adsorbed H atoms play the role of anchoring the CO_2 molecules, by reducing them. The nature of the first electroreduced product is unknown, although an ensemble of CO_2, H_2O and H_{ad} has been postulated [7]. Thus, the electroadsorption process for Pt can be formulated as

$$CO_2\,(aq) \longleftrightarrow CO_2\,(\text{interphase}) \quad [1]$$

$$CO_2\,(\text{interphase}) + H_{ad} + H_2O \longleftrightarrow \left[CO_2 . H_{ad} . H_2O\right] \quad [2]$$

It has been shown that H adatoms located at (110) sites have the highest activity toward CO_2 electro-reduction [18]. This fact was also demonstrated by performing potential perturbations in a medium frequency range (2-20 Hz) within the potential domain for H electrosorption on (110) sites. Furthermore, H atoms adsorbed on terraces (100) can reduce CO_2 at the interphase, probably forming $(CO)_{ad}$ in a bridge configuration,

$$CO_2\,(\text{interphase}) + 2H_{ad} \longleftrightarrow (CO)_{ad} + H_2O \quad [3]$$

A different situation arises for Rh. The fact that the adsorbates formed on Rh are more reduced than CO suggests that CO_2 can be dissociatively adsorbed, as already found in the solid/gas interphase [19,20]

$$CO_2\,(aq) \longleftrightarrow (CO)_{ad} + O_{ad} \quad [4]$$

and these adsorbates are reduced in the hydrogen potential region.

Electroreduction of the adsorbates initially formed

H atoms participating of the ensemble built on Pt at $E \leq E_{pzc}$ are able to reduce CO_2 producing subsequently formiate species,

$$\left[CO_2 . H_{ad} H_2O\right] \longleftrightarrow \left(COOH\right)_{ad} + H_2O \quad [5]$$

The voltammetric results indicate that another adsorbed residue has been formed. The application of the MFPR in the OH-electrosorption potential domain allows to suggest that both adsorbates, namely $(COOH)_{ad}$ and $(CO)_{ad}$, could be interrelated through an equilibrium involving $(OH)_{ad}$ species according to

$$(COOH)_{ad} \longleftrightarrow (CO)_{ad} + (OH)_{ad} \quad [6]$$

The prevalence of either $(COOH)_{ad}$ or $(CO)_{ad}$ depends on the time during which the adsorption potential is applied. Thus, short times favour the formation of $(COOH)_{ad}$ over $(CO)_{ad}$, but prolonged adsorption potentials account for the formation of most stable species, i.e., $(CO)_L$ if H atoms are adsorbed at Pt(110) sites or$(CO)_B$ if H atoms are adsorbed at Pt (100) sites.

For Rh electrodes and according to DEMS results, a combination of three-coordinated (COH) and formyl type (COH) adsorbates can be proposed.

Relationship between the adsorbates: surface equilibrium

The main consequence of the application of the MFPR is focused on the variation of the interatomic Pt–Pt distance, which can be almost certainly responsible of a change in the CO configuration, namely, CO_L changes into CO_B. This should indicate that $(COOH)_{ad}$ and $(CO)_L$ adsorbates are probably linked through an equilibrium involving $(CO)_B$ species,

$$(COOH)_{ad} \longleftrightarrow \left[(CO_L)_{ad} + (OH)_{ad}\right] \quad [7]$$

And

$$(CO)_L \longleftrightarrow (CO)_B \quad [8]$$

In this sense, the formation of $(CO)_B$ is favoured after the application of the MFPR.

Electrooxidation of the adsorbates

Carbon dioxide is the oxidation product formed both on Pt and Rh. Formiate can be oxidized at a potential more negative than that of OH-electrosorption reaction. Thus, the electrooxidation can be described as

$$(COOH)_{ad} \longleftrightarrow CO_2 + H^+ + e^- \quad [9]$$

For $(CO)_{ad}$, both in bridge and lineal configurations, the electrooxidation involves the previous adsorption of OH species on the free surface sites, according to

$$Pt + H_2O \longleftrightarrow Pt(OH)_{ad} + H^+ + e^- \quad [10]$$

which further oxidizes the adsorbates as follows

$$(CO)_{ad} + (OH)_{ad} \longleftrightarrow CO_2 + H^+ + e^- \quad [11]$$

The electro-oxidation process involves both reactions meaning that 2 electrons are exchanged.

On Rh the adsorbates are also oxidized by $(OH)_{ad}$ species,

$$(COH)_{ad} + (OH)_{ad} \longleftrightarrow CO_2 + 2H^+ + 2e^- \quad [12]$$

and then, the global electrooxidation reaction involves 3 electrons.

Conclusions

Carbon dioxide interacts with Pt and Rh electrodes in aqueous sulphuric acid through a complex mechanism that involves several stages keeping a strong dependence on the substrate.

For Pt, CO_2 interacts with H adatoms and interfacial water molecules, forming a complex that is subsequently adsorbed. The formation of this complex is assisted by H adatoms located either at (110) or (100) sites. This complex is electro-reduced to $(COOH)_{ad}$ which is in equilibrium with $(OH)_{ad}$ and $(CO_L)_{ad}$ or with $(OH)_{ad}$ and $(CO_B)_{ad}$. These configurations link up with the H adatom surface location, i.e., $(CO_L)_{ad}$ is favoured by (110) sites whereas $(CO_B)_{ad}$ by (100) sites.

For the case of Rh, CO_2 is adsorbed in a dissociated fashion leaving CO as a strongly adsorbed residue which is subsequently hydrogenated to $(COH)_{ad}$. This adsorbate is strongly bound to the surface. Both adsorbates, $(COOH)_{ad}$ on Pt or $(COH)_{ad}$ on Rh are electrooxidized to CO_2.

Acknowledgements

This work was partially financed by the ANPCyT PICTR /0188 (Argentina). Author acknowledges Dr. Carlos Fernando Zinola Sánchez, Dr. Eduardo Méndez Morales (Universidad de la República, Uruguay), Dr. Elena Pastor, Dr. José Luis Rodríguez and Dr. Carmen Arévalo (Universidad de La Laguna, España) for DEMS facilities and helpful discussions. MEM is a member of CONICET-UNLP.

References

[1] Corrigan D.; M.J. Weaver, *J. Electroanal. Chem.* **1988**, *241*, 143.
[2] Kunimatsu K.; Lezna R.O.; M. Enyo, *J. Electroanal. Chem.* **1989**, *258*,115.
[3] Chang S.C.; Weaver M.J., *J. Electroanal. Chem.* **1990**, *285*, 263.
[4] Chang S.C.; Weaver M.J., *Surf. Sci.* **1990**, *238*, 142.
[5] Westerhoff B.; R. Holze, *Ber. Bunsenges. Phys. Chem.* **1993**, *97*, 418.
[6] Méndez E.; Martins M.E.; C.F. Zinola, *J. Electroanal. Chem.* **1999**, *477*, 41.
[7] Arévalo M.C.; Gomis-Bas C.; Hahn F.; Beden B.; Arévalo A.; Arvia A.J., *Electrochim. Acta* **1994**, *39*, 793.
[8] Taguchi S.; A. Aramata, *Electrochim. Acta* **1994**, *39*, 2533.
[9] Nikolic B.Z.; Huang H.; Gervasio D.; Lin A.; Fierro C.; Adzic R.R.; E.B. Yeager, *J. Electroanal. Chem.* **1990**, *295*, 415.

[10] Rodes A.; Pastor E.; T. Iwasita, *J. Electroanal. Chem.* **1994**, *373*, 167.
[11] Rodes A.; Pastor E.; T. Iwasita, *J. Electroanal. Chem.* **1994**, *369*, 183.
[12] Rodes A.; Pastor E.; T. Iwasita, *J. Electroanal. Chem.* **1994**, *377*, 215.
[13] Sun S.G.; Clavilier J.; Bewick A., *J. Electroanal. Chem.* **1988**, *240*, 147.
[14] Nichols R.J.; A. Bewick, *Electrochim. Acta* **1988**, *33*, 1691.
[15] Iwasita T.; Nart F.C.; López B.; W. Vielstich, *Electrochim. Acta* **1992**, *37*, 2361.
[16] Willsau J.; Heitbaum J., *Electrochim. Acta* **1986**, *31*, 943.
[17] Silva-Chong J.; Méndez E.; Rodríguez J.L.; Arévalo M. C.; Pastor E., *Electrochim. Acta* **2002**, *47*, 1441.
[18] Hoshi N.; Mizumura T.; Hori H., *Electrochim. Acta* **1995**, *40*, 883.
[19] van Tol M.F.H.; Gielbert A.; B.E. Nieuwenhuys, *Appl. Surf. Sci.* **1993**, *67*, 166.
[20] van Tol M.F.H.; Gielbert A.; Wolf R.M.; Lie A.B.K.; B.E. Nieuwenhuys, *Surf. Sci.* **1993**, *287/288*, 201.
[21] Arévalo C.; Gomis-Bas C.; F. Hahn, *Electrochim. Acta* **1998**, *44*, 1369.
[22] Furuya N.; Shibata M., *J. Electroanal. Chem.*, **1999**, *467*, 85.
[23] Electrochemical and Electrocatalytic Reactions of Carbon Dioxide, Elsevier, 1993.
[24] Jitaru M.; Lowy D.A.; Toma M.; Toma B.C.; I. Oniciu, *J. Appl. Electrochem.* **1997**, *27*, 875.
[25] Encyclopedia of Electrochemistry of the Elements, Editor A. J. Bard, Marcel Dekker, Inc., New York., 1976.